Acta Crystallographica Section B
**Structural Science**
ISSN 0108-7681

# Solid-state and gas-phase structures of two conformers of *N*-(4-methylphenyl)-*N*′,*N*″-bis(morpholinyl) phosphoric triamide; insights from X-ray crystallography and DFT calculations

**Khodayar Gholivand* and Hamid Reza Mahzouni**

Department of Chemistry, Tarbiat Modares University, PO Box 14115-175, Tehran, Iran

Correspondence e-mail: gholi_kh@modares.ac.ir

Received 9 November 2010
Accepted 21 March 2011

A phosphoric triamide with the formula (4-$CH_3$—$C_6H_4NH$)P(O)($NC_4H_8O$)$_2$ has been synthesized and characterized. X-ray crystallography at 120 K reveals that the title compound is composed of two symmetrically independent molecules in the solid state. Density functional theory (DFT) calculations reveal that two conformers *A* and *B* are very close to each other from an energy point of view. Thus there is equal chance that the presence of two conformers in the lattice may lead to hydrogen-bonded chains with an *ABABAB* arrangement. Hydrogen bonds of the type $O_P\cdots H-N$ ($O_P$ being the phosphoryl O atom) are established between the two conformers with binding energies of −18.8 and −20.3 kJ mol$^{-1}$ (at B3LYP/6–31+G*). The electronic delocalization LP($O_P$) → $\sigma^*$(N—H), LP($O_P$) being the lone pair of $O_P$, leads to a decrease in the strength of the N—H bond during hydrogen bonding between the conformers. The charge density ($\rho$) at the bond critical point (b.c.p.) of N—H decreases by ∼ 0.012–0.014 e Å$^{-3}$ when the molecule participates in hydrogen bonding. This may explain the red shift of the $\nu$(N—H) stretching frequency from a single molecule in the gas phase to a hydrogen-bonded one in the solid state.

## 1. Introduction

Phosphoric triamides have been extensively investigated as stereoselective catalysts (Denmark & Fu, 2001; Denmark *et al.*, 2006), urease (Andrews *et al.*, 1986; Domínguez *et al.*, 2008) and acetylcholinesterase inhibitors (Bollinger *et al.*, 1990; Gholivand, Shariatinia, Khajeh & Naderimanesh, 2006), and efficient complexant molecules for lanthanides (Gholivand, Mahzouni & Esrafili, 2010; Gholivand, Mahzouni, Pourayoubi & Amiri, 2010). The ring inversion and rotation of cyclic amines around the P—N bond produce different conformers in phosphoric triamides (Corbridge, 1995; Gholivand, Alizadehgan *et al.*, 2006). Such compounds with two (Gholivand & Pourayoubi, 2004; Gholivand *et al.*, 2005), three (Cain *et al.*, 2003; Gholivand *et al.*, 2009) and four (Gholivand, Vedova, Firooz *et al.*, 2005; Gholivand, Shariatinia & Pourayoubi, 2006) conformers have been previously reported. The conformational diversity in these compounds leads to a wide range of hydrogen bonds (Gholivand, Vedova, Firooz *et al.*, 2005; Gholivand, Shariatinia & Pourayoubi, 2006). It is well known that the physicochemical properties of compounds depend on the presence of intermolecular hydrogen bonds (Pankratov & Shalabay, 2007, and references therein). The analysis of hydrogen bonding is helpful to rationalize the structural and physicochemical properties of compounds. In previous works we have performed a conformational analysis of phosphoric triamides (Gholivand, Vedova, Firooz *et al.*, 2005; Gholivand *et al.*, 2009). Moreover, we have recently investigated the

**Table 1**
Crystallographic data of the compound.

| | |
|---|---|
| Crystal data | |
| Chemical formula | $C_{15}H_{24}N_3O_3P$ |
| $M_r$ | 325.34 |
| Crystal system, space group | Monoclinic, $P2_1/n$ |
| Temperature (K) | 120 |
| $a, b, c$ (Å) | 9.517 (3), 10.723 (3), 32.993 (8) |
| $\beta$ (°) | 96.029 (6) |
| $V$ (Å$^3$) | 3348.3 (16) |
| $Z$ | 8 |
| Radiation type | Mo $K\alpha$ |
| $\mu$ (mm$^{-1}$) | 0.18 |
| Crystal size (mm) | 0.50 × 0.15 × 0.05 |
| Data collection | |
| Diffractometer | Bruker *SMART* 1000 CCD area detector |
| Absorption correction | – |
| No. of measured, independent and observed [$I > 2\sigma(I)$] reflections | 16 054, 6459, 3369 |
| $R_{int}$ | 0.068 |
| Refinement | |
| $R[F^2 > 2\sigma(F^2)]$, $wR(F^2)$, $S$ | 0.051, 0.119, 0.87 |
| No. of reflections | 6459 |
| No. of parameters | 407 |
| No. of restraints | 0 |
| H-atom treatment | H-atoms treated by a mixture of independent and constrained refined |
| $\Delta\rho_{max}$, $\Delta\rho_{min}$ (e Å$^{-3}$) | 0.42, −0.36 |

electronic and steric effects of *para* substituents on the conformational diversity and hydrogen bonding of phosphoric triamides of the formula (4-*X*-$C_6H_4NH$)P(O)($NC_5H_{10}$)$_2$, *X* = F, Cl, Br, H and $CH_3$ (Gholivand & Mahzouni, 2011). In the present study two conformers of the compound (4-$CH_3$—$C_6H_4NH$)P(O)($NC_4H_8O$)$_2$ are introduced. The solid-state structure of the compound was determined by X-ray crystallography and employed as a reference for quantum mechanical (QM) calculations at the B3LYP level. The electronic aspects of the hydrogen bonds in the crystalline compound were investigated by natural bonding orbital (NBO) and atoms in molecules (AIM) analyses.

## 2. Experimental

### 2.1. Synthesis of *N*-4-methylphenyl-*N*′,*N*″-bis(morpholinyl) phosphoric triamide

All chemicals were purchased commercially and used without further purification. The intermediate *N*-(4-methylphenyl) phosphoramidic dichloride was prepared according to literature procedures (Gholivand *et al.*, 2001). A solution of 4 mmol morpholine in dry acetonitrile (30 ml) was then added dropwise to a stirred solution of 1 mmol *N*-(4-methylphenyl) phosphoramidic dichloride at 268 K. After stirring for 5 h the solvent was evaporated under vacuum. The white product was washed with distilled water and recrystallized from a mixture of methanol and water. The synthesis pathway for the compound is represented below.

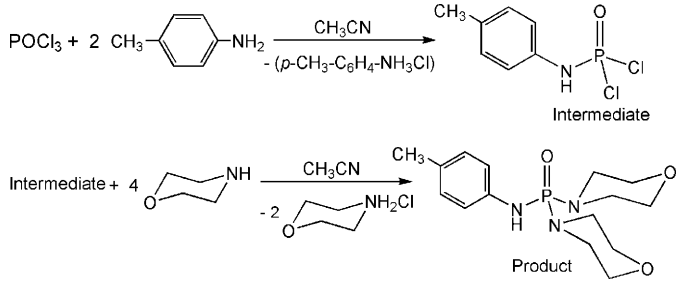


Yield: 70%, m.p. 459 K. IR (KBr, cm$^{-1}$): 3150 (s), 2845 (s), 1607 (w), 1505 (s), 1444 (m), 1279 (m), 1252 (m), 1190 (s, P═O), 1129 (s), 1103 (s), 962 (s), 806 (w), 718 (w), 473 (m). $^1$H NMR ($CDCl_3$, 500.13 MHz, 298 K): $\delta$ 2.27 (s, 3H, $CH_3$), 3.18 (m, 8H, $CH_2$), 3.59 (m, 8H, $CH_2$), 3.95 [d, $^2J$(PNH) = 8.2 Hz, 1H, NH], 7.00 [d, $^3J$(H,H) = 8.4 Hz, 2H, Ar-H], 7.04 [d, $^3J$(H,H) = 8.4 Hz, 2H, Ar-H]. $^{13}$C NMR ($CDCl_3$, 125.76 MHz, 298 K): $\delta$ 20.59 (s, *p*-$CH_3$), 45.09 (s, $CH_2$), 67.12 [d, $^3J$(P,C) = 5.5 Hz, $CH_2$], 118.73 [d, $^3J$(P,C) = 6.2 Hz, $C_{ortho}$], 129.83 (s), 131.59 (s), 137.43 (s). $^{31}$P NMR ($CDCl_3$, 202.46 MHz, 298 K): $\delta$ 11.41 (m).

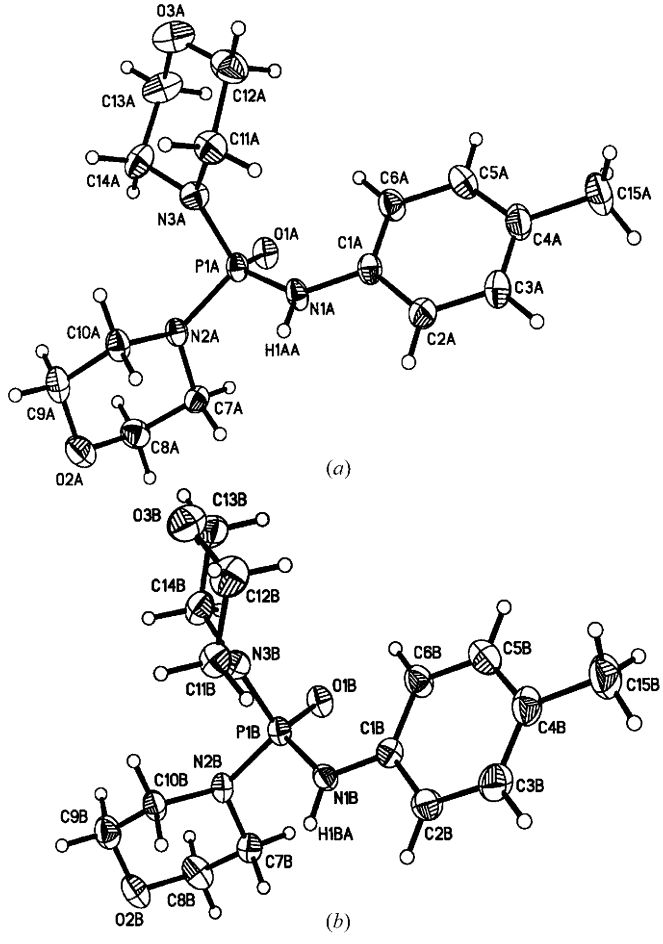


**Figure 1**
Displacement ellipsoid plot (at the 50% probability level) and atom-labeling of two conformers (*a*) *A* and (*b*) *B*.

**Table 2**
Selected bond lengths (Å), charge densities ($\rho$) and vibrational data of conformers *A* and *B*.

| | X-ray | 6-31G* | 6-31+G* | 6-311+G* | $\rho$† at the b.c.p. (e Å$^{-3}$) | Vibrational frequency | |
|---|---|---|---|---|---|---|---|
| Parameter | *A*/*B* | *A*/*B* | *A* = *B* | *A* = *B* | *A*/*B* | Experimental | Calculated†‡ |
| P═O | 1.478 (2)/1.477 (2) | 1.491/1.489 | 1.492 | 1.487 | 0.224/0.225 | 1190 vs | 1234 |
| P—N1 | 1.635 (2)/1.634 (2) | 1.697/1.694 | 1.694 | 1.691 | 0.166/0.167 | 962 s | 913 |
| P—N2 | 1.630 (2)/1.643 (3) | 1.687/1.686 | 1.676 | 1.672 | 0.174/0.173 | 1103 s | 972 |
| P—N3 | 1.652 (2)/1.653 (2) | 1.691/1.675 | 1.688 | 1.683 | 0.173/0.175 | 1103 s | 978 |
| N1—H1 | – | 1.014/1.012 | 1.013 | 1.009 | 0.328/0.328 | 3150 s | 3589 |

† The values have been calculated at the B3LYP/6-31+G* level for fully optimized conformers *A* and *B*. ‡ Without factor scale correction.

### 2.2. Instrumentation

$^{1}$H, $^{13}$C and $^{31}$P NMR spectra were recorded on a Bruker Avance DRX 500 spectrometer. $^{1}$H and $^{13}$C chemical shifts were determined relative to an internal TMS standard, and $^{31}$P chemical shifts relative to 85% $H_3PO_4$ as an external standard. IR spectra were recorded on a Shimadzu model IR-60 spectrometer using KBr pellets. Melting points were obtained with an electrothermal instrument.

### 2.3. Crystal structure determination

Single crystals of the compound were obtained from a mixture of $CH_3OH/H_2O$ at room temperature. X-ray data were collected on a Bruker (1998) SMART 1000 CCD area detector with graphite-monochromated Mo $K\alpha$ radiation ($\lambda$ = 0.71073 Å) and refined by full-matrix least-squares methods against $F^2$ with *SHELXL*97 (Sheldrick, 2008). The H atoms of the NH groups were objectively localized in the difference Fourier syntheses and refined in isotropic approximation. The H(C) atoms were placed in calculated positions and included in the refinement within a riding model with fixed isotropic displacement parameters [$U_{iso}$(H) = 1.2$U_{eq}$(C*i*) or 1.5$U_{eq}$(C*ii*) for methyl groups]. $U_{eq}$(C*i*,C*ii*) values are the equivalent isotropic displacement parameters of the C atoms to which the corresponding H atoms are bonded. The crystallographic data of the studied compound are summarized in Table 1.[1] An *ORTEP* view of the compound is shown in Fig. 1.

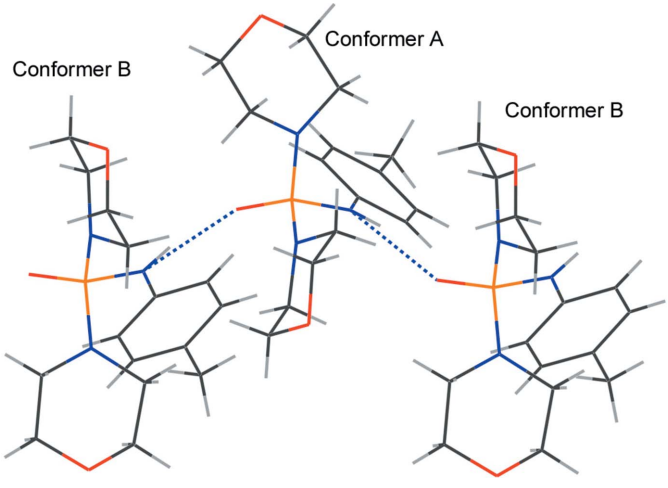


**Figure 2**
Model hydrogen-bonded cluster *BAB* for DFT calculations, in which the target molecule is in the center. A similar model was considered for the cluster *ABA*, in which conformer *B* in the center is the target molecule.

### 2.4. Computational details

The solid-state structure was used as a starting point for the DFT calculations in the gas phase. The conformers were modeled as hydrogen-bonded clusters *BAB* and *ABA* in which the target conformer is surrounded by two neighbors (Fig. 2). As X-ray crystallography cannot accurately determine the position of the H atoms, optimization of the H-atom positions was performed at the B3LYP/6-31G* level for the model clusters, while other atoms were kept frozen. We denote these structures as hydrogen-optimized systems. Moreover, conformers *A* and *B* were fully optimized as single molecules in a vacuum, with 6-31G*, 6-31+G* and 6-311+G* basis sets. The NBO (Reed *et al.*, 1988) and AIM (Bader, 1990, 1991) analyses were carried out at the B3LYP/6-31+G* level for both monomers and model clusters. Moreover, a vibrational analysis was also performed for fully optimized monomers at the B3LYP/6-31+G* level. The geometry and electronic features of the isolated conformers were compared with those of clusters. The hydrogen-binding energies have been calculated, based on the equation $\Delta E_{HB} = E_{dimer} - E_A - E_B$, where HB is hydrogen bonding, $E_A$ refers to conformer *A* and $E_B$ refers to conformer *B*, and then were corrected for basis set superposition error (BSSE) using the counterpoise method (Boys & Bernardi, 1970). All quantum chemical calculations have been carried out using the *GAUSSIAN*98 package (Frisch *et al.*, 1998).

## 3. Results and discussion

### 3.1. NMR investigation

$^{31}$P{$^{1}$H}NMR at room temperature shows a single resonance at 11.41 p.p.m., indicating that the title compound presents only one conformer in solution. We have previously shown that low-temperature NMR experiments are unable to indicate if such compounds exhibit more conformers in solution, owing to solubility problems (Gholivand & Mahzouni, 2011). The $^{1}$H NMR spectrum exhibits a doublet at 3.95 p.p.m. with $^{2}J_{PH}$ = 8.2 Hz for the amidic proton. Two doublets at 67.12

[1] Supplementary data for this paper are available from the IUCr electronic archives (Reference: SO5046). Services for accessing these data are described at the back of the journal.

**Table 3**
Hydrogen-bonding data for the X-ray structure and model clusters.

The values in brackets refer to the calculated distances (at B3LYP/6-31G*), charge densities, delocalization energies and binding energies (at B3LYP/6-31+G*) for model clusters. The others refer to the X-ray structure.

| | | | | | $\rho$ at the b.c.p. (e Å$^{-3}$) | | | |
|---|---|---|---|---|---|---|---|---|
| $D$—H···$A$ | $d$(N—H) | $d$(H···O) | $d$(N···O) | ∠NHO | N—H | H···O | $E^{(2)}$† | $\Delta E_{HB}$‡ |
| N1$A$—H1$A$···O1$B^{i}$ | 0.880 [1.025] | 1.922 [1.753] | 2.778 (3) | 163.7 [179.3] | [0.314] | [0.037] | [108.7] | [−20.3] |
| N1$B$—H1$B$···O1$A^{ii}$ | 0.880 [1.024] | 1.936 [1.782] | 2.802 (3) | 167.8 [173.8] | [0.316] | [0.034] | [95.3] | [−18.8] |

Symmetry codes: (i) $-x+1, -y+1, -z+1$; (ii) $-x, -y+1, -z+1$. † The stabilizing energy $E^{(2)}$ in kJ mol$^{-1}$ for the LP(O$_P$)$_i$ → $\sigma^*$(N—H)$_j$ electronic delocalization. ‡ The binding energy in kJ mol$^{-1}$ for O$_A$···H$_B$—N$_B$ and O$_B$···H$_A$—N$_A$ hydrogen bonds.

($^3J_{PC}$ = 5.5 Hz) and 118.73 ($^3J_{PC}$ = 6.2 Hz) p.p.m. in the $^{13}$C NMR spectrum are related to methylene and *ortho* C atoms, respectively.

### 3.2. Structural analysis

As shown in Fig. 1 the title compound contains two conformers, *A* and *B*, that differ slightly from each other in the steric orientation of one of the morpholine rings. In previous work (Gholivand & Mahzouni, 2011) it has been shown that the rotation of amine groups around the P—N bonds produces various conformers in a similar compound, *para*-CH$_3$—C$_6$H$_4$NHP(O)(NC$_5$H$_{10}$)$_2$. However, the P═O and P—N bond lengths in the central unit O═P(N1)(N2)(N3) of conformer *A* are very close to those of conformer *B*. The selected bond lengths are given in Table 2. The P═O distances are 1.478 (2) and 1.477 (2) Å for conformers *A* and *B*. Similar trends are observed in the case of P—N bonds except for P1—N3. It seems that the difference between P1*A*—N3*A* [1.630 (2) Å] and P1*B*—N3*B* [1.643 (3) Å] bond lengths is correlated to the various orientations of morpholine rings. For instance, the O1—P1—N3—C14 torsion angle is 52.9 (3) and 44.9 (2)° in conformers *A* and *B*. In both conformers *A* and *B* the P═O bond and the phenyl ring are in a *gauche* conformation. The torsion angle O1—P1—C1—C6 is 46.5 and 46.1° in conformers *A* and *B*. The crystal lattice of the compound contains one-dimensional zigzag hydrogen-bonded chains with an *ABABAB* arrangement which are produced by the N—H···O$_P$ (O$_P$ being the phosphoryl O atom) hydrogen bonds. These strong hydrogen bonds are established in this compound with different donor–acceptor distances of 2.778 (3) and 2.802 (3) Å (Table 3).

### 3.3. Fully optimized conformers in the gas phase

In order to compare the geometry and energy aspects of conformers *A* and *B* they have been separately optimized as single molecules in vacuum. The optimized geometries were confirmed to be the minimum energy point with no imaginary vibrations. The optimized conformers *A* and *B* at B3LYP/6-31G* are very close to each other from energy and structural points of view. The energy difference between the two conformers is 1.1 kJ mol$^{-1}$. The most equality is found in the central unit O═P(N1)(N2)(N3) for two conformers *A* and *B*. This similarity may lead to an equal chance for conformers *A* and *B* to produce an *ABABAB* arrangement in the hydrogen-bonded chain. The calculated P═O, P—N and N—H distances have been represented in Table 2 for two conformers. The two conformers convert to a unique structure when larger basis sets are used. However, Table 2 shows that the change in basis set used for geometry optimizations has no significant effect on the measure of structural parameters. Based on the results of AIM and NBO analyses we found that the optimized structures with 6-31G* basis sets are more appropriate to describe the electronic structure of the compound. Thus the latter structures have been used to perform further analyses and are discussed in the text.

As shown in previous work, the weak intramolecular CH···O$_P$ hydrogen bond between the *ortho*-proton of the phenyl and the phosphoryl O atom creates a six-membered ring *via* the O1—P1—N1—C1—C6—H6 bond paths. This intramolecular contact stabilizes a *gauche* configuration between the P═O bond and the phenyl ring (Gholivand & Mahzouni, 2011). Here, the aforementioned *gauche* configuration is seen, whereas the torsion angle O1—P1—C1—C6 is 6.7 and 33.4° for conformers *A* and *B*, respectively. A stabilization energy $E^{(2)}$ of 3.3 kJ mol$^{-1}$ (at B3LYP/6-31+G*) has been previously reported (Gholivand & Mahzouni, 2011) for the LP(O$_P$) → $\sigma^*$(C—H$_{ortho}$) electronic delocalization in a similar compound with a piperidine ring instead of morpholine. Here, at the same level, the stabilization energies $E^{(2)}$ of 12.2 and 2.7 kJ mol$^{-1}$ have been calculated for the LP(O$_P$) → $\sigma^*$(C—H$_{ortho}$) interaction in conformers *A* and *B*, respectively. The charge density ($\rho$) values at the bond critical point (b.c.p.) of the CH$_{ortho}$···O$_P$ contact are 0.00161 and 0.0098 e Å$^{-3}$ for conformers *A* and *B*.

### 3.4. Electronic parameters of the hydrogen-bonded clusters

The charge densities at the b.c.p.s and stabilization energies $E^{(2)}$ of the LP(O$_P$) → $\sigma^*$(N—H) electronic delocalization together with the calculated and X-ray parameters of hydrogen bonds are presented in Table 3 for hydrogen-optimized clusters. Whereas the optimization was performed only for H-atom positions, the donor–acceptor distances for hydrogen bonds in hydrogen-optimized clusters are equal to those from the experimental data. The NBO analysis reveals that the electronic delocalization LP(O$_P$)$_i$ → $\sigma^*$(N—H)$_j$ is established during hydrogen bonding between the subunits *i* and *j* within the clusters. Such an electronic density transfer results in weakening of the N—H bond. The measure of

stabilizing energies $E^{(2)}$ for this electronic delocalization can be used to characterize the strength of the donor–acceptor interactions in hydrogen bonding (Esrafili *et al.*, 2008). Here the stabilizing energies $E^{(2)}$ of 95.3 and 108.7 kJ mol$^{-1}$ have been calculated for LP($O_P$) $\rightarrow$ $\sigma^*$(N—H) electron-density transfer in $O_A\cdots H_B—N_B$ and $O_B\cdots H_A—N_A$ hydrogen bonds. It should be noted that the stabilizing energies $E^{(2)}$ differ from the hydrogen-bonding energy. The former refers to the stabilization energy of the electron delocalization between donor–acceptor orbitals. The hydrogen-bonding energy is related to the sum of the total attractive and repulsive forces between two hydrogen-bonded fragments. Here the hydrogen-bonding energies have been calculated on the basis of the energy difference between the hydrogen-bonded dimer *AB* and its monomers. The hydrogen-bonding energy values of −18.8 and −20.3 kJ mol$^{-1}$ were obtained at B3LYP/6-31+G* for $O_A\cdots H_B—N_B$ and $O_B\cdots H_A—N_A$ hydrogen bonds . Table 3 shows that the $\rho$ value at the b.c.p. of the O$\cdots$H contact increases from the $O_A\cdots H_B—N_B$ hydrogen bond (0.034 e Å$^{-3}$) to $O_B\cdots H_A—N_A$ (0.037 e Å$^{-3}$), in line with a decrease in the donor–acceptor distance.

### 3.5. Vibrational spectrum

The calculated P—N distances are relatively large compared with those of the X-ray structure. Thus the calculated $\nu$(P—N) stretching modes (in the 913–978 cm$^{-1}$ region) are significantly lower than those of the experimental values. In the cases of P═O and N—H bonds, although the P═O and N—H distances in fully optimized conformers are longer than those of the solid-state structure, the calculated $\nu$(P═O) and $\nu$(N—H) modes, 1234 and 3589 cm$^{-1}$, are larger than those obtained in the experimental spectra (1190 and 3150 cm$^{-1}$). It should be mentioned that the P═O and N—H bonds in the solid-state structure are directly involved in hydrogen bonding. The $\rho$ values at the b.c.p. of the N—H bonds decrease from 0.328 e Å$^{-3}$ in fully optimized monomers *A* and *B* (Table 2) to 0.314–0.316 e Å$^{-3}$ in model clusters (Table 3). At the same level, a similar shift (0.328 to 0.316 e Å$^{-3}$) in the $\rho$ value at the b.c.p. of N—H bonds has also been reported for *para*-$CH_3—C_6H_4NHP(O)(NC_5H_{10})_2$ in previous work (Gholivand & Mahzouni, 2011). The mean N—H distance increases from 1.013 Å in isolated conformers to 1.025 Å in hydrogen-bonded clusters. Intermolecular hydrogen bonding can be responsible for lengthening the N—H bond from the fully optimized to hydrogen-bonded clusters. This may explain the red shift of the $\nu$(N—H) stretching mode from the calculated values to the experimental spectrum. Although the calculated vibrational frequencies differ slightly from experimental values, no scale factor was used to correct the calculated vibrational modes. The differences between the calculated and experimental values have also been observed in previous studies on similar compounds (Iriarte *et al.*, 2008; Gholivand *et al.*, 2008, 2009, 2011), which is normally attributed to the packing effects in solid-state structures.

## 4. Conclusions

The title compound contains two independent conformers in the solid phase that are very close to each other from structural and energy viewpoints. Rotation of the amine groups around the P—N bonds produces two conformers and results in two NH$\cdots$$O_P$ hydrogen bonds with different donor–acceptor distances. Unlike the $\nu$(P—N) modes, the $\nu$(P═O) and $\nu$(N—H) stretching frequencies decrease significantly from the calculated ones for fully optimized conformers to the experimental values, owing to the participation of P═O and N—H bonds in hydrogen bonding and packing effects in the solid-state structure. The results of NBO and AIM analyses revealed that the electronic delocalization LP($O_P$) $\rightarrow$ $\sigma^*$(N—H) leads to a decrease in the strength of the N—H bond, while the $\rho$ value at the b.c.p. of N—H decreases comparatively from the isolated conformers to hydrogen-bonded clusters. This may explain the red shift of the $\nu$(N—H) stretching mode from the calculated values to the experimental spectrum.

Financial support of this work by Research Council of Tarbiat Modares University is gratefully acknowledged.

## References


Andrews, R. K., Dexter, A., Blakeley, R. L. & Zerner, B. (1986). *J. Am. Chem. Soc.* **108**, 7124–7125.

Bader, R. F. W. (1990). *Atoms in Molecules: A Quantum Theory*. Oxford University Press.

Bader, R. F. W. (1991). *Chem. Rev.* **91**, 893–928.

Bollinger, J. C., Levy-serpier, J., Debord, J. & Penicaut, B. (1990). *J. Enzyme Inhib. Med. Chem.* **3**, 211–217.

Boys, S. F. & Bernardi, F. (1970). *Mol. Phys.* **19**, 553–566.

Bruker (1998). *SMART*, Version 5.059. Bruker AXS, Madison, Wisconsin, USA.

Cain, M. J., Cawley, A., Sum, V., Brown, D., Thornton-Pett, M. & Kee, T. P. (2003). *Inorg. Chim. Acta*, **345**, 154–172.

Corbridge, D. E. C. (1995). *Phosphorus, an Outline of its Chemistry, Biochemistry and Technology*, 5th Ed. Amsterdam: Elsevier.

Denmark, S. E. & Fu, J. (2001). *J. Am. Chem. Soc.* **123**, 9488–9489.

Denmark, S. E., Pham, S. M., Stavenger, R. A., Su, X., Wong, K. T. & Nishigaichi, Y. (2006). *J. Org. Chem.* **71**, 3904–3922.

Domínguez, M. J., Sanmartín, C., Font, M., Palop, J. A., San Francisco, S., Urrutia, O., Houdusse, F. & García-Mina, J. (2008). *J. Agric. Food Chem.* **56**, 3721–3731.

Esrafili, M. D., Behzadi, H. & Hadipour, N. L. (2008). *Theor. Chem. Acc.* **121**, 135–146.

Frisch, M. J. *et al.* (1998). *GAUSSIAN*98, Revision A.7. Gaussian Inc., Pittsburgh PA, USA.

Gholivand, K., Alizadehgan, A. M., Arshadi, S. & Firooz, A. A. (2006). *J. Mol. Struct.* **791**, 193–200.

Gholivand, K., Ghadimi, S., Naderimanesh, H. & Forouzanfar, A. (2001). *Magn. Reson. Chem.* **39**, 684–688.

Gholivand, K. & Mahzouni, H. R. (2011). *Polyhedron*, **30**, 61–69.

Gholivand, K., Mahzouni, H. R. & Esrafili, M. D. (2010). *Theor. Chem. Acc.* **127**, 539–550.

Gholivand, K., Mahzouni, H. R., Pourayoubi, M. & Amiri, S. (2010). *Inorg. Chim. Acta*, **363**, 2318–2324.

Gholivand, K., Mostaanzadeh, H., Koval, T., Dusek, M., Erben, M. F. & Della Védova, C. O. (2009). *Acta Cryst.* B**65**, 502–508.

Gholivand, K. & Pourayoubi, M. (2004). *Z. Anorg. Allg. Chem.* **630**, 1330–1335.

Gholivand, K., Shariatinia, Z., Khajeh, K. & Naderimanesh, H. (2006). *J. Enzyme Inhib. Med. Chem.* **21**, 31–35.
Gholivand, K., Shariatinia, Z. & Pourayoubi, M. (2005). *Z. Naturforsch. B*, **60**, 67–74.
Gholivand, K., Shariatinia, Z. & Pourayoubi, M. (2006). *Polyhedron*, **25**, 711–721.
Gholivand, K., Vedova, C. O. D., Erben, M. F., Mahzouni, H. R., Shariatinia, Z. & Amiri, S. (2008). *J. Mol. Struct.* **874**, 178–186.
Gholivand, K., Vedova, C. O. D., Firooz, A. A., Alizadehgan, A. M., Michelini, M. C. & Diez, R. P. (2005). *J. Mol. Struct.* **750**, 64–71.
Iriarte, A. G., Erben, M. F., Gholivand, K., Jois, J. L., Ulic, S. E. & Vedova, C. O. D. (2008). *J. Mol. Struct.* **886**, 66–71.
Pankratov, A. N. & Shalabay, A. V. (2007). *J. Struct. Chem.* **48**, 427–432.
Reed, A. E., Curtiss, L. A. & Weinhold, F. (1988). *Chem. Rev.* **88**, 899–926.
Sheldrick, G. M. (2008). *Acta Cryst.* A**64**, 112–122.